

The Effect of Residual Stress on Coupling Power Loss of VCSEL Modulus

Jao-Hwa Kuang¹, Chao-Ming Hsu², Ah-Der Lin³, Jyun-Wei Luo³

1.Dept. of Mech. and Electro-Mech. Engr., National Sun Yat-Sen Univ.,
kuang@faculty.nsysu.edu.tw

2.Dept. of Mech. Engr., National Kaohsiung Univ. of App. Sci.,
jammy@cc.kuas.edu.tw

3.Dept. of Mech. Engr., Cheng-Shiu Univ., ader@csu.edu.tw
Kaohsiung, Taiwan

Abstract. In this article, the effect of residual stress on active region misalignment of laser light sources for vertical cavity surface emitting laser (VCSEL) modulus has been studied. The post-weld-shift variation of active region introduced from the residual stress distribution variation for different VCSEL solder joints, i.e. tin-silver (Sn/3.5Ag) and tin-lead (Sn/37Pb) solder joints, are simulated by employing the thermal-elastic-plastic finite element model of MARC package. The ball grid solidification in reflow process and the creep deformation in the acceleration aging were simulated and analyze. The time and temperature dependent material properties of solders are employed. Numerical results indicate that the post-weld-shift introduced from residual stress in the solidification process are significant, and are also the key reasons to reduce the coupling efficiency in VCSEL packaging. The non-sequential components models in commercial Zemax optical package were used to estimate the optical coupling power loss between the active region and the fiber tip in VCSEL modulus. The results show that the proposed post-weld-shift model is feasible to analyze and to improve the solder joint design in the VCSEL packaging.

Keywords: VCSEL, FEM , Creep , residual stresses, misalignment.

1. Introduction

Manufactured by GeAs, the VCSEL modulus is an active opto-electronic device, and quite different from traditional laser diodes [1]. It has a compact volume coupled with fiber by circle beam, and is made in an arrayed form for better fiber communications [2] [3]. The optical coupled power of a VCSEL modulus depends upon residual stress distribution and the corresponding PWS (post-weld shift) after the reflow process [4]. To ensure the reliability of the VCSEL modulus for temperature-fluctuating operations, the endurance tests are necessary and versatile [5]. The notable item is the acceleration aging test. In the test, the thermal stresses dominate the VCSEL modulus deformation which induces the active region misalignment for VCSEL. The misalignment has a strong influence on the optical coupled power loss [6]. Basically, the VCSEL modulus is classified into three parts; VCSEL structure, micro-solder ball and silicon bench (substrate), as shown in figure 1. The dimensions of VCSEL modulus are 4200x1200x2400 μm . The sizes of a VCSEL structure are 1000x300x265.5 μm . In the opto-electronic packaging, solder surface mounted technology (SMT) is used to connect the components [7]. To assemble the VCSEL modulus, SMT uses different solder ball joints, such as Sn/37Pb and Sn/3.5Ag solders. Of particular interest, the pad design is the layout for laser sources, layers mounting markers, and solder ball positioning, etc.

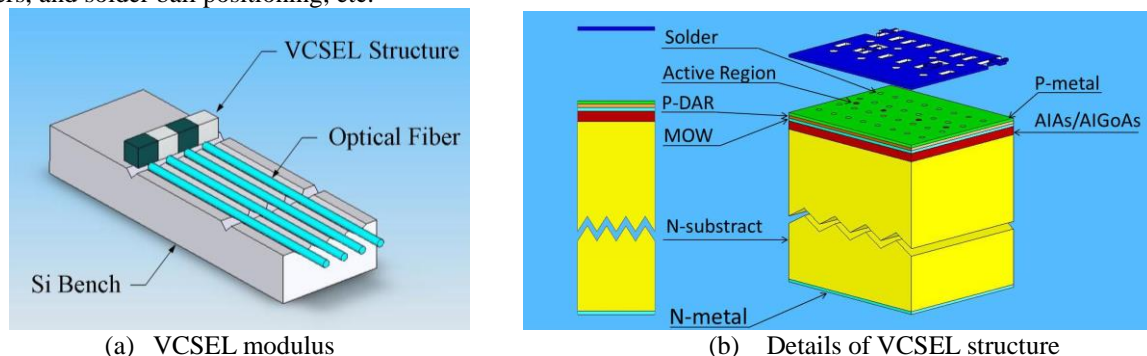


Fig.1 Schematic illustrations of VCSEL

In this study, both Sn/37Pb and Sn/3.5Ag solders are simulated. The residual stresses for both solders are calculated for the reflow process and acceleration aging test. The coefficient of thermal expansion (CTE) of GaAs is two times as that of silicon. Due to the CTE difference between GaAs and Si, the residual stress has great influence on the yielding and misalignment of VCSEL. The effect of creeping is included in the acceleration aging test. The active region misalignment induced by the residual stress will be investigated for evaluating the optical coupled power loss for VCSEL.

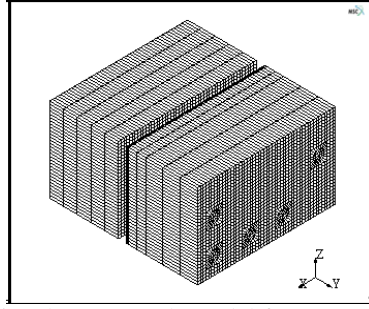


Fig.2 Finite element mesh model for VCSEL modulus

2. Finite element model for VCSEL modulus

Surface Evolver simulating the solder solidification process is used to predict the shape of solder during the reflow process. The reflowed solder shape will be reconstructed in the finite element package of *MSC, MARC*. Figure 2 shows the VCSEL mesh model symmetric about yz-plane. The substrate is made of pure silicon and its sizes are 1000x300x250 μm . The node number is 12480 for VCSEL structure, 960 for micro-solder ball, and 7800 for substrate, respectively. The laser sources in the VCSEL structure indicated by points A are located at the center of the active region, as shown in figure 1 (b). The primary composition of VCSEL structure consists of GaAs, Au, Pt and Ti. Considering the creeping effects, the power of first order is included in this study[8].

On the boundary, the nature convection coefficient for a local area was proposed by Ellison [9] based upon experimental method. Table 1 lists the experience factors of the nature convection coefficient having a value of zero on the symmetric surface. The nature convection coefficient can be written as below.

$$h = 2.79k (\Delta T/L)^m \quad (\text{W/m}^2 \cdot ^\circ\text{C})$$

where h is the nature convention coefficient, ΔT the temperature difference between boundary and environment($^\circ\text{C}$), m the first experience factor, k the second experience factor, and L the characteristic length(m). Furthermore, the corners of yz-plane (the symmetric plane) are fixed, and the other points of yz-plane have no displacement in the x-direction. The material of VCSEL modulus follows the isotropic-hardening rule, von-Mises yielding criterion, and Prandtl-Reuss flow rule. The optical coupled power loss of VCSEL modulus is estimated by Zemax using its powerful non-sequential module. The roughness of the reflection surface is close to the quality of mirror, and the maximum clear aperture is 50 μm . Each laser source diode contains 1000 layout rays and 50000 analysis rays of 8mW.

Table 1 Experience factors for convection by Ellison [10]

Char. Plane.	L	k	m
Vertical plane	height	1.22	0.35
Horizontal plane (face up)	a	1.0	0.35
Horizontal plane(face down)	a	05	0.33

Note: $a = \text{length} \times \text{width} / 2 \times [(\text{length} + \text{width})]$

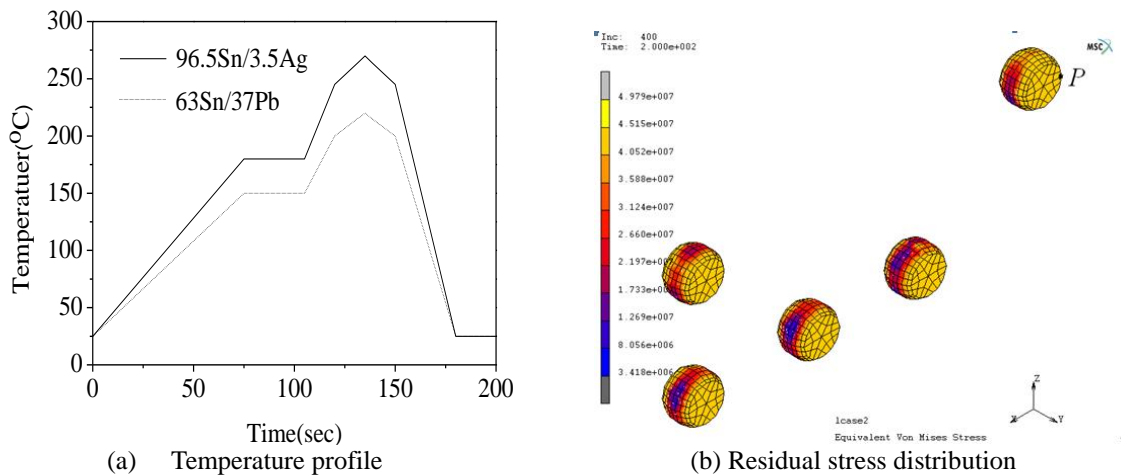


Fig.3 Reflow process for VCSEL using Sn/37Pb solder joints.

3. Numerical results and discussion

In the simulation, the process sequence is the reflow process followed by the acceleration aging test. The temperature profile of the reflow process is shown in figure 3(a). The time period for a VCSEL modulus is 3 minutes in the reflow process. According to Bellcore standard TA-TSA- 000983, the acceleration aging test in this study has a temperature of 85 $^\circ\text{C}$ maintained for 5000 hours. The residual stress distribution is then calculated and the corresponding

displacement of VCSEL modulus is then estimated. The mechanic-thermal coupled field is adopted in the numerical analysis.

The joints of VCSEL structure use Sn/37Pb or Sn/3.5Ag solder ball. The solder ball joint has a significant effect on the misalignment of the active region in view of deformation induced by the residual stresses. Figure 3(b) presents the residual stress distribution of Sn/37Pb solder joints used by the VCSEL modulus for the reflow process. After the reflow process, the maximum von Mises stresses is 28 Mpa and its position is marked by point P. It is found that point P is located at the interface between the solder joint and the pad, as shown in figure 3(b). As shown in figure 4, the stress variation of point P is calculated for the reflow process and the acceleration aging test which follows the reflow process. It is observed that the stress of point P is close to zero at the melting point of Sn/37Pb solder. In the solidification stage, the stress of point P rises up and finally come to a fixed value, the residual stress of point P. Similarly, the residual stress is 45.8 Mpa for Sn/3.5Ag solder joint. According to figure 4 (b), the stress relaxing caused by creeping is obvious.

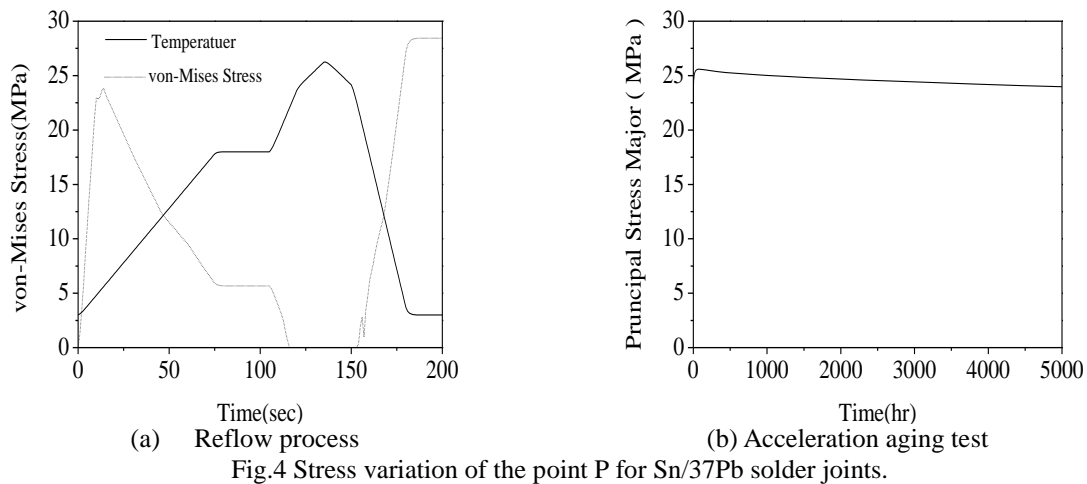


Fig.4 Stress variation of the point P for Sn/37Pb solder joints.

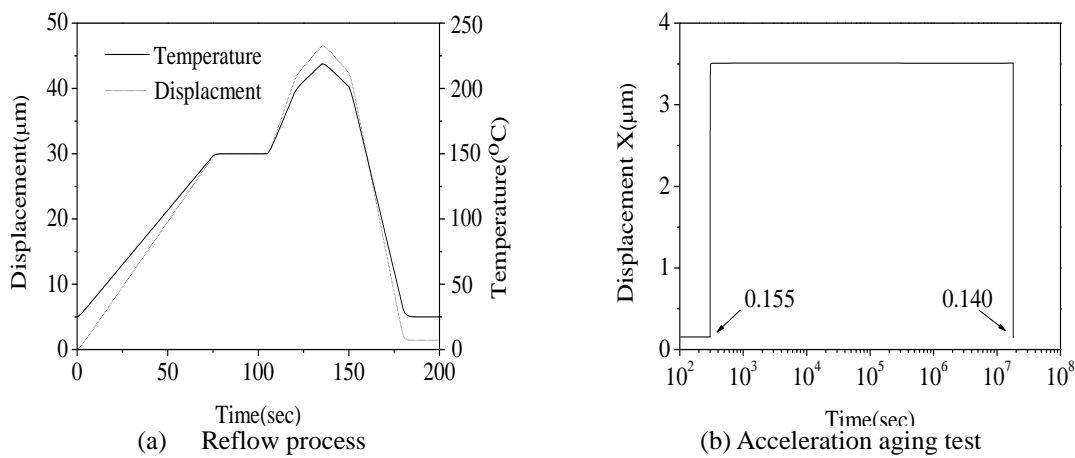


Fig.5 Displacement of point A of VCSEL using Sn/37Pb solder joints

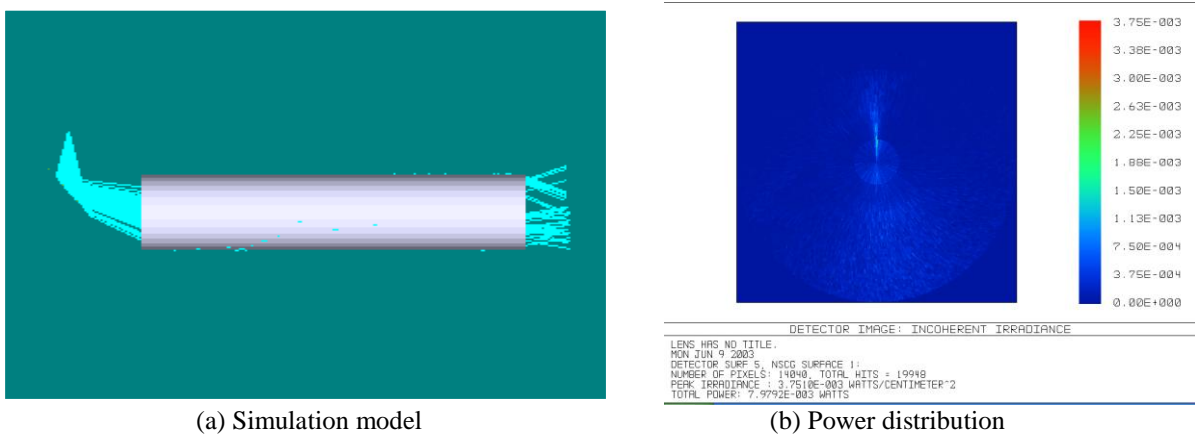


Fig. 6 Simulation of Zemax

As shown in figure 6, the optical coupled power loss is simulated by Zemax. The fiber material is BK7, 125μm diameter and 4200μm length. The core material is SF11 with 40μm diameter and 4200μm long. In industry, the initial alignment of the VCSEL structure and fiber is set to have the greatest power transmitting efficiency. Then followed by

the reflow process, the VCSEL structure and fiber are jointed. Generally, the optical coupled power loss will increase for each process or test. According to the numerical simulation, the center of the active region, point A, has the greatest PWS. The displacement and the corresponding optical coupled power loss are listed in table 2. According to the table, the displacement changes from 0.155 μm to 0.140 μm for the Sn/37Pb solder joints, and from 0.212 μm to 0.184 μm for the Sn/3.5Ag. However, the optical coupled power loss increases from 0.25% to 4% for the Sn/37Pb solder, and 1.875% to 5% for the Sn/3.5Ag solder.

Table.2 Active region displacement (μm)/ Optical coupled power loss for different solder ball grid array joints

Solder materials	Sn/37Pb	Sn/3.5Ag
Reflow Process only	0.155 / 0.25%	0.212 / 1.875%
Reflow Process +Aging test	0.140 / 4%	0.184 / 5%

4. Conclusions

In this study, the residual stress distribution and the deformation for Sn/37Pb and Sn/3.5Ag ball grid array of VCSEL were investigated. The corresponding optical coupled power loss was estimated by the displacement from the finite element analysis. The simulated results reveal that both the post-solder-shift and the creep deformation may affect the coupling efficiency significantly. However, due to the high melting point, the Sn/3.5Ag ball grid array joint always provide the better coupling efficiency than the Sn/37Pb joint during the acceleration aging test.

References

- [1] Melanie Ott, Harry Shaw, September 21, 2001, "Evaluation of Vertical Cavity Emitting Lasers (VCSEL) mounted on Diamond Substrates," NASA/GSFC Component Technology and Radiation Effects Branch.
- [2] H. Roscher and R. Michalzik, "Low thermal resistance flip-chip bonding of 850 nm 2-D VCSEL arrays capable of 10 Gbit/s/ch operation", in Proc. IEEE Lasers and Electro-Opt. Soc. Ann. Meet., LEOS 2003, vol. 2, pp. 511–512. Tucson, AZ, USA, Oct. 2003
- [3] R. Michalzik, R. King, R. Jäger, S. Müller, and K.J. Ebeling, "VCSEL arrays for CMOS integrated optical interconnect systems" (invited), in Optoelectronic and Wireless Data Management, Processing, Storage, and Retrieval, R. Raymond, P.K. Srimani, R. Su, and C.W. Wilmsen (Eds.), Proc. SPIE 4534, pp. 101–113, 2001.
- [4] Anderson, T. ,Guven, I., Madenci, E., and Gustafsson, G, 2000, "The Necessity of Reexamining Previous Life Prediction Analysis of Solder Joints in Electronic Packages," IEEE, PP. 516-520.
- [5] Pardeep K. B., Klaus G., Kwang, A. Y., and Ahmer R. S., 1995, "Three-Dimensional Creep Analysis of Solder Joints in Surface Mount Devices," Transactions of the ASME, vol.117 pp.20-25.
- [6] Amagai, M., 1999, "Characterization of Chip Scale Packaging Materials," Microelectronics Reliability, Vol. 39, pp. 1365-1377.
- [7] Zarrow, P., 2000, soldering, SMT 101,pp.80-86.
- [8] Lau, J. H. and Pao , Y. H., 1997, Solder Joint Reliability of BGA, CSP, Flip Chip, and Fine Pitch SMT Assemblies, McGraw-Hill, New York, USA.
- [9] Ellison, Gordon N., Thermal Computations for Electronic Equipment, Robert E. Krieger Publishing Co., Malabar, Florida, 1989.